MAGNETIC BUNCHERS FOR THE GENERATION OF HIGH PEAK CURRENT, LOW EMITTANCE ELECTRON PULSES AT MEDIUM ENERGY*

B. E. Carlsten, B. D. McVey, and E. M. Svaton,**
G. R. Magelssen, and L. M. Young
MS H825, Los Alamos National Laboratory, Los Alamos, NM 87545

Introduction

A goal of many electron accelerator systems is high peak current, low emittance, and low energy spread. This is particularly useful for Free-Electron Laser (FEL) devices,[1] but is also beneficial for other uses.[2] In Fig. 1 we see typical FEL performance as a function of peak current, emittance, and energy spread. Unfortunately, these goals are basically contradictory. As the peak current is increased, the space charge forces also increase, and the emittance due to nonlinear space charge forces grows. There has been significant improvement in the design of photoelectric injectors which minimizes the emittance growth due to space-charge forces,[3] but in general the normalized 90% emittance scales as:

$$\epsilon_{90\%norm}^2 = r_o^4\left(1+\tau_b^2 k_2^2\right)^2 + \left(\frac{k_3 eQ}{2m\epsilon_o \pi\sqrt{z^2+4r_o^2}}\right)^2$$

where

$$z = \frac{mc^2}{eE}\left(\sqrt{1+\tau_b^2\frac{e^2E^2}{m^2c^2}}-1\right)$$

and Q is the bunch charge, e is the electronic charge and m its mass, E is the accelerating gradient at the cathode, r_o is the initial beam radius, and τ_b is the duration of the laser pulse. The constants k_1, k_2, and k_3 depend on the exact design of the photoinjector, but typically lead to a dependence like

$$\epsilon_{90\%norm} = 10 + 5\frac{Q}{\sqrt{1+\left(\frac{z}{2r_o}\right)^2}}$$

where Q is in nanoCoulombs and the units of emittance are π mm mrad.

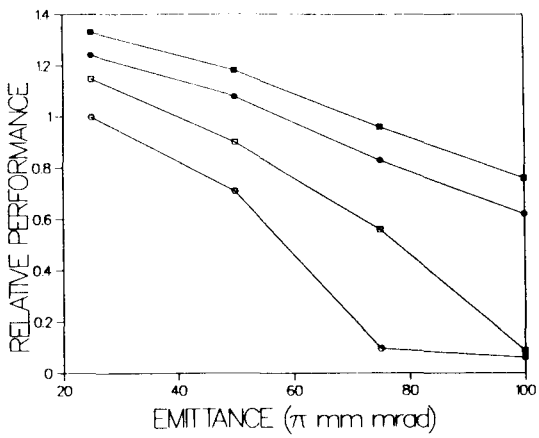

Fig. 1. FEL performance as a function of emittance. Squares are for 0.5% energy spread and circles are for 0.8% energy spread. Solid symbols are for 625 A and open symbols are for 375 A.

We see two effects from this scaling. First, for vanishingly short pulses, the emittance does not increase past a certain value for a given charge because the radial space charge force remains finite. Next we see that if the pulse length is increased, the emittance contribution due to the space charge drops.

*Work supported and funded by the US Department of Defense, Army Strategic Defense Command, under the auspices of the US Department of Energy.
**Rockwell International, Rocketdyne Division.

Sufficient motivation arises from this scaling to start with a long pulse length (until the rf effects cannot be ignored) and then bunch the beam to the desired peak current. If possible, this bunching should be done at a high enough energy so the reduced space charge forces will not lead to additional emittance growth. This bunching is provided by a transport section with magnetic dispersion. Bunching occurs if the correct energy-phase correlation is impressed on the bunch, typically by dephasing the rf fields slightly from the maximum energy gain of the beam.[4,5] The emittance growth of previous designs roughly obey

$$\Delta\epsilon_{90\%norm}(\pi \text{ mm mrad}) = 25\frac{I}{\gamma^2}$$

where the current I is in Amperes.[5] In this paper we will discuss new types of magnetic bunchers with one third the emittance growth, allowing bunching to 1KA at medium energy (20 to 40 MeV) with emittance increases of less than 10 π mm mrad, added in quadrature.

We will also consider in this paper the effects of limited rf power. In general, it is always preferable to bunch at as high an energy as possible, but under certain limitations[6] this cannot be done. In the next section, we will outline the various physical constraints and issues for magnetic buncher design. Discussion of achromatic design and dispersion and minimizing rf power will be presented.

In the following section we will provide generic designs for positive and negative dispersion. A short section will follow describing the effect of curvature in the energy-phase correlation due to the sinusoidal nature of the rf fields on the output pulse shape. Methods to remove the curvature will be examined. The final section will cover simple nonlinear dispersion which can compensate for the curvature.

General Considerations

In this section, the basic ideas for magnetic buncher design will be discussed. First, geometric and chromatic aberrations must be avoided. The concepts of linear and higher order dispersion are introduced. Next, the curvature in the energy slew will be discussed. Finally, the emittance growth in the bunchers due to space charge forces will be examined. After these items are introduced, we will discuss specific magnetic bunchers and comparisons of them. Space charge forces are ignored until the end of the section.

To second order, the magnetic field in a dipole can be expressed as[7]

$$B_y(x,0,\Delta s) = B_y(0,0,\Delta s)(1-nhx+\beta_c h^2 x^2)$$

where h is the inverse bending radius $\frac{qB_y}{mc\beta\gamma}$, n is the field gradient, β_c is the field curvature term, and Δs is the path variable within the dipole, for a dipole with field in the transverse y direction. A general analysis of the electrons' behavior in the dipoles must include a description of the transfer matrix R with field gradient n and field curvature β_c. However, since we will look at the transport from a geometrical basis and there are several complete descriptions available,[7,8] it will not be included here. From this theory, multiple dipoles are required for any magnetic system to eliminate chromatic aberrations.

In Fig. 2 we see an example of a type of a magnetic buncher called the chicane, which provides geometrical and chromatic symmetry. This is true of a larger class of bunchers which has pairs of parallel pole faces. Any transverse displacement of the beam yields an equal final transverse displacement. Initial transverse velocities produce final displacements linear with the initial velocity (for small velocities), and the velocity is preserved. The buncher

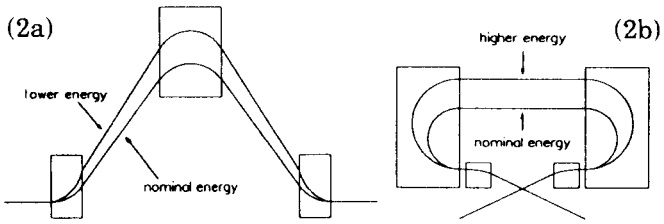

Fig. 2. Configuration of the chicane (a) and circular (b) bunchers.

essentially looks like a drift to the beam. The chicane buncher has some nonlinear dispersion, even with constant gradient dipoles.

These properties are inherent with symmetric designs with parallel pole faces,[9] and we will only discuss this class of bunchers. This allows us to neglect the R matrix analysis, until we use nonzero field gradients in a later section. Another variant of the parallel pole face idea is also shown in Fig. 2, called the circular buncher. This design has only linear dispersion with zero field gradients.

The cavities after the buncher must be phased to eliminate the energy slew required for bunching. Let W_1 and N_1 be the maximum energy gain per cavity and the number of cavities before the buncher, and W_2 and N_2 be them after the buncher. The angle ϕ_1 and ϕ_2 are the rf phases the center of the bunch sees before and after the buncher. If θ_1 is the pulse phase length before the buncher and θ_2 after the buncher, then the energy spread ΔW satisfies

$$\Delta W = 2N_1W_1\cos\phi_1\sin\frac{\theta_1}{2} \qquad (1a)$$

$$\Delta W = -2N_2W_2\cos\phi_2\sin\frac{\theta_2}{2}. \qquad (1b)$$

The curvature, or deviation from a straight line, for the energy slew is

$$\Delta W_c = N_1W_1\left(\cos\phi_1\left(\sin\theta_1 - \theta_1\right) - \cos\theta_1\sin\phi_1\right) \quad . \qquad (2)$$

We see that this is increased with increased pulse length θ_1, and has a maximum for ϕ_1 near $\frac{\pi}{2}$. The curvature is greatest for the larger dispersion bunchers, and longer initial pulse lengths. Without compensating for the nonlinear dispersion in the buncher, this results in a skewed final current profile. Usually this is not desirable, and can lead to significant emittance growth during the rest of the transport.

Assuming that the emittance growth for nonlinear optics and the fringe fields are eliminated, the emittance growth from a buncher is due only to the space charge forces. In particular, there are axial and radial forces within the bend. The predominate effect is when the forces change the kinetic energy of a particle while it is still within the buncher, destroying the achromaticity of the buncher. The axial force changes the energy, inversely proportional to gamma. It can be made quite small by decreasing the path length or operating at a higher energy. The radial force creates a potential redistribution of the particles as the beam bunches, and the energy change is independent of gamma. Usually this is small, but can dominate if the other effect is reduced enough. These effects can be minimized by focusing the beam to a waist in the final dipole.[9]

In order to compare these effects, we should in principle compare the rms potential change of the beam. However, the resulting algebra and complicated expressions mask the underlying physics, and we will make scaling arguments from simple formulas. The voltage change from the axial space charge force is very dependent on the actual longitudinal density distribution. The initial distribution is somewhat parabolic. This allows for an axial force throughout the pulse; if the initial distribution is square, the voltage change is primarily located at the axial ends. The emittance growth scales as the energy change divided by the energy. The potential redistribution is also dependent on the longitudinal density distribution, although in all cases it is distributed along the entire length of the pulse.

The resulting emittance is of a different nature from the two effects. The emittance growth from the axial space charge force arises from a twist in phase space for different axial locations in the pulse; the emittance at a single axial location is quite small. On the other hand, the emittance from the potential redistribution effect appears as a radial twisting in the phase space for all axial slices.

The space charge field at a point from a transverse disk of charge Δz away, where r_o is the disk's radius, and ρ is the charge density, is

$$\Delta E_z = \frac{\rho}{2\epsilon_o}\left(1 - \sqrt{\frac{\Delta z^2}{\Delta z^2 + r_o^2}}\right) \quad . \qquad (3)$$

It is easy to check that this expression reduces in the limit Δz is zero to the surface field from Gauss's law, and in the limit r_o is zero to Coulomb's formula for a point charge.

Integrating this expression for a uniform slug of charge, we find that the axial field at the ends of the slug is (to lowest order in $\frac{r_o}{z_o}$):

$$E_{z,rest} = \frac{Q}{4\pi\epsilon_o r_o z_o}, \qquad (4)$$

for a pulse length of z_o. This axial field is in the beam's rest frame, and

$$z_o = \gamma\beta c\tau_b \quad .$$

Using

$$E_{z,lab} = E_{z,rest} \quad ,$$

the resulting voltage change for the ends of the pulse after a drift of length ΔS is then

$$\Delta V = \frac{Q\Delta S}{4\pi\epsilon r_o\tau_b\gamma\beta c} \quad . \qquad (5)$$

For an accurate answer, we should integrate over the path ΔS in the buncher as τ_b decreases, but as an approximate answer, we can assume ΔS is roughly one quarter of the path length in the buncher and τ_b is the final pulse length. Since the voltage change is mostly at the axial ends, we will write for it

$$\Delta V = F\frac{Q(\Delta S/4)}{4\pi\epsilon r_o\tau_{b,final}\gamma\beta c} \qquad (6)$$

where F is a form factor, less than one.

The relative voltage change from the potential redistribution of the center of the beam (for a uniform beam) is given by

$$\Delta V = \frac{Q}{4\pi\epsilon_o\beta c}\left(\frac{1}{\tau_{b,final}} - \frac{1}{\tau_{b,initial}}\right) \quad , \qquad (7)$$

where $\tau_{b,final}$ and $\tau_{b,initial}$ are the final and initial pulse lengths. Assuming that the initial pulse is long, we equate Eqs. 6 and 7 to see at what buncher path length the two effects are of the same size

$$\Delta S = 4\gamma r_o\frac{1}{F} \quad .$$

For beam sizes around 2.5 mm, energies of 20 MeV, and using a form factor of 0.5, we see that the axial space charge effect becomes smaller than the potential redistribution for path lengths less than 80 cm. This is of course just a rough estimate, but it indicates that we should try to design bunchers with path lengths well under one meter.

Examples of Positive and Negative Dispersion Bunchers

In this section, we will compare the circular and chicane bunchers. For equal path lengths, the circular buncher has about three times the dispersion and that its dispersion is positive, while the chicane has negative dispersion. For geometrical reasons, positive dispersion bends usually have more dispersion.

The dispersion of the circular buncher is completely linear, but there is some nonlinear dispersion for the chicane. This is because the rotation angle caused by the first dipole is not linear with energy but instead satisfies the transcendental equation

$$L\theta = \Delta S\sin\theta$$

where L is the width of the dipole and ΔS is the path length in it. Because the particles' paths in the dipoles of the circular buncher are circles sliced into two and displaced, there is no nonlinearities in its transport. It looks like a drift to the beam.

In Fig. 3 we see the emittance increase as a function of energy for both bunchers. The smaller emittance introduced with the circular buncher is due to its larger dispersion and shorter path length. Emittance diagnostics indeed show that the emittance growth is dominated by the potential redistribution.

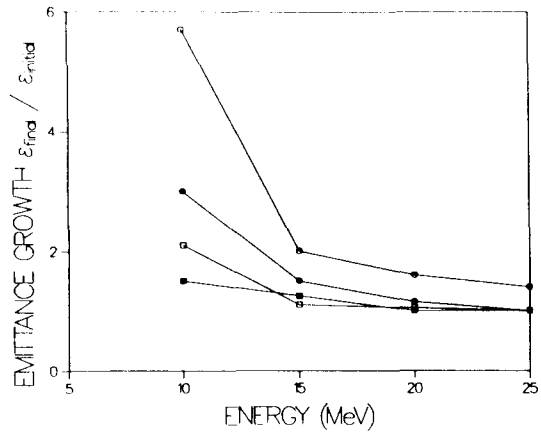

Fig. 3. Transverse emittance growth for bunching 8 nC from 160 to 500 A for the chicane (open symbols) and circular (solid symbols) bunchers at different energy. Squares are for horizontal emittance, and circles are for vertical emittance.

Effects of the Curvature of the RF

In Fig. 4 we see the initial parabolic and final skewed current profiles before and after the circular buncher. The units of phase are degrees at 433 MHz. The skewing is from the curvature in the energy phase slew, also shown in Fig. 4. This skewed output current profile is undesirable. The curvature can be removed before the start of the buncher. A conventional approach is to use a third harmonic rf cavity.[10] Another technique is to use a series of wake-field producing apertures or other disturbances. The initial current profile is typically cosine-like shaped from the initial axial space-charge forces in the first cavity. The wake potential lags somewhat behind the current profile, but if the lag is short relative to the length of the pulse, the energy-phase slew can be significantly straightened.

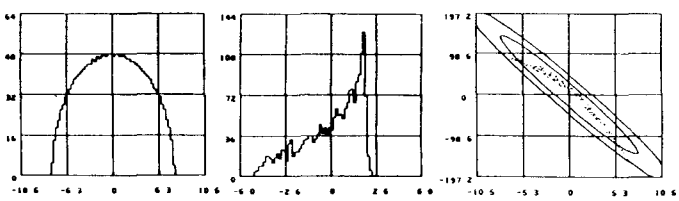

(4a) (4b) (4c)

Fig. 4. Initial current profile (a) and after bunching (b) for the circular buncher. Energy slew is shown in (c).

Alternatively, nonlinear dispersion in the dipoles from nonzero field gradients or field curvature can compensate for the energy slew curvature. In Fig. 5 we see an example generated by angling the pole faces apart. The path length in the dipoles is now a nonlinear function of a particle's energy.

Conclusion

We have presented a class of magnetic bunchers which have parallel pole faces. This symmetry reduces or eliminates

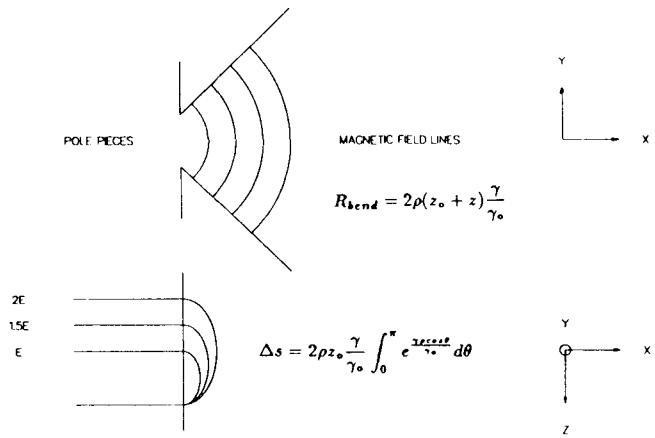

Fig. 5. Simple nonlinear dispersion in the circular buncher can be provided by separating the pole faces at an angle, reducing the magnetic field for the higher energy particles.

geometrical and chromatic aberrations, and leads to smaller emittance growth than with conventional designs. We have further divided this class into two subclasses, those with positive and those with negative dispersion. The positive dispersion designs have larger dispersion and smaller emittance growth, but the smaller energy spread results in a larger curvature in the energy-phase slew. This curvature results in a skewed output current profile. The curvature can be removed before the bend either by rf or by space charge forces. If it is not removed, nonlinear dispersion in the bend can be added, which corrects the pulse profile, but may introduce small geometrical aberrations.

References

1. J. C. Goldstein, B. E. Carlsten, and B. D. McVey, "INEX Simulations of the Los Alamos HIBAF Free-Electron Laser MOPA Experiment," Proc. 11th Int. Free-Electron Laser Conf., Naples, Florida, Aug. 1989, to be published.
2. J. B. Murphy and C. Pellegrini, Preface, Proc. ICFA Workshop on Low Emittance e^--e^+ Beams, Brookhaven Natl. Lab., March 1987, BNL report 52090.
3. B. E. Carlsten,"Photoelectric Injector Design Code," Proc. 1989 IEEE Particle Accelerator Conf., IEEE Catalog No. 89CH2669-0, 133 (1989).
4. B. E. Carlsten and K. C. D. Chan, "Preliminary Injector, Accelerator, and Beamline Design for RF-Linac-Driven XUV Free Electron Lasers," *Nucl. Instrum. Meth. Phys. Res.* **A272**, 208 (1988).
5. T. I. Smith,"Summary of the Working Group on Electron Linac Guns," Proc. ICFA Workshop on Low Emittance e^--e^+ Beams, BNL, March 1987, BNL report 52090.
6. B. E. Carlsten, R. L. Sheffield, and B. D. McVey, "Photoelectric Injector Designs at Los Alamos National Laboratory," Proc. ICFA Workshop on Short Pulse High Current Cathodes, Bendor, France, June 1990, to be published.
7. K. R. Crandall, "TRACE 3-D Documentation," Los Alamos Report LA-11054-MS.
8. D. C. Carey, R. V. Servranckx, and K. L. Brown, "Second-Order Path Length Terms for a General Bending Magnet," Particle Accelerators **13**, 199 (1983).
9. L. M. Young, Los Alamos National Laboratory, private communication.
10. K. C. D. Chan and J. S. Fraser, "Minimum Beam-Energy Spread of a High-Current RF Linac," Proc. 1987 IEEE Particle Accelerator Conf., IEEE Catalog No. 87CH2387-9, 1075 (1987).